



# NeQuick-G performance assessment for space applications

Oliver Montenbruck<sup>1</sup> · Belén González Rodríguez<sup>1,2</sup>

Received: 29 August 2019 / Accepted: 2 November 2019 / Published online: 19 November 2019  
© The Author(s) 2019

## Abstract

Other than traditional single-layer ionosphere models for global navigation satellite system (GNSS) receivers, the NeQuick-G model of Galileo provides a fully three-dimensional description of the electron density and obtains the ionospheric path delay by integration along the line of sight. While optimized for users on or near the surface of the earth, NeQuick-G can thus as well be used for ionospheric correction of single-frequency observations from spaceborne platforms. Based on slant and total electron content measurements obtained in the Swarm mission, the performance of NeQuick-G for users in low earth orbit is assessed for periods of high and low solar activity as well as different orientations of the orbital plane with respect to the sun and the region of high total electron content. A slant range correction performance of better than 70% is achieved in more than 85% of the examined epochs in good accord with the performance reported for terrestrial users. Likewise, the positioning errors can be notably reduced when applying the NeQuick-G corrections in single-frequency navigation solutions. For users at orbital altitudes, it is furthermore shown that vertical total electron predictions from NeQuick-G may be favorably combined with an elevation-dependent thick-layer mapping function to reduce the high computational effort associated with the integration of the electron density along the ray path for each tracked GNSS satellite.

**Keywords** NeQuick · Low earth orbit · Ionosphere · Mapping function · Swarm · Galileo

## Introduction

The use of GNSS receivers is nowadays a well-established technique for positioning, navigation and timing on satellites in low earth orbit (LEO). At representative altitudes of 400–1400 km, these satellites are still located in the terrestrial service volume. The signal strength and visibility conditions are generally similar to those of terrestrial users and enable similar real-time navigation performances as well as geodetic-grade precise orbit determination in post-processing (Montenbruck 2017).

The orbital height of LEO satellites is typically at or above the ionospheric electron density maximum. As such, single-frequency receivers that are widely used for

spacecraft platform operations with accuracy requirements of few to 10 m can benefit from reduced ionospheric path delays compared to receivers close to the surface of the earth. On the other hand, most of the real-time ionospheric correction models for terrestrial single-frequency GNSS users (Klobuchar 1987; Jakowski et al. 2011; Yuan et al. 2019) cannot directly be applied for space users. These models are typically designed to provide a global description of the vertical total electron content (VTEC) based on a limited number of parameters that are updated routinely based by the service provider. The slant total electron content (STEC) and thus the range delay in these models are then obtained by multiplication with an elevation-dependent mapping function based on a single-layer, thin-shell approximation.

For LEO users, the common ionospheric correction models lack an altitude-dependent description of the total electron content above the orbit as well as a suitable mapping function that accounts for the structure of the ionosphere at altitudes of 400 km and up. This is illustrated in Fig. 1, which shows examples of electron density profiles for regions of high and low total electron content. Obviously, a thin-layer approximation is no longer meaningful for users above the peak height, where the electron density

---

✉ Oliver Montenbruck  
oliver.montenbruck@dlr.de  
Belén González Rodríguez  
belen.grmm@gmail.com

<sup>1</sup> Deutsches Zentrum für Luft- und Raumfahrt, German Space Operations Center, 82234 Wessling, Germany

<sup>2</sup> Present Address: ESA/ESTEC, Keplerlaan 1, 2200 AG Noordwijk, The Netherlands

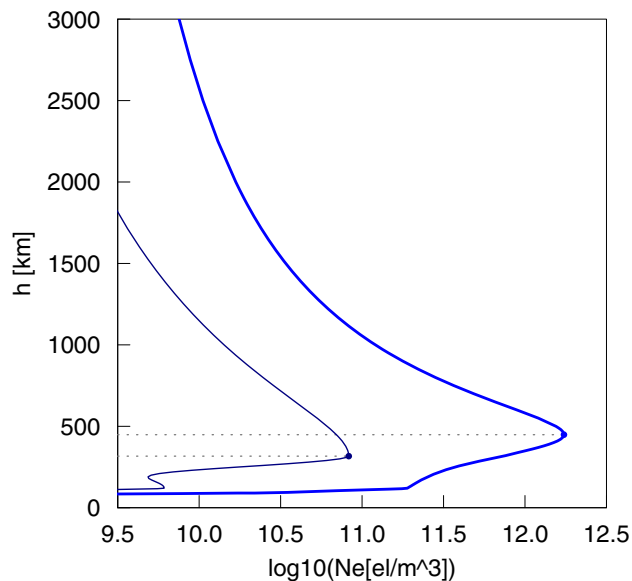


**Fig. 1** Examples of electron density profiles based on the NeQuick-G model for mid-January 2014 at a location on the equator at local noon (bold line) and at 60° northern latitude at local midnight (thin line). Dotted lines indicate the corresponding heights of the F-layer density maximum

shows a roughly exponential decrease with altitude. Likewise, the variation of electron density with altitude does not allow to establish a generic model for the  $VTEC(h)/VTEC(h=0)$  ratio of space- and ground-based total electron content that might be used to scale the predictions of terrestrial ionosphere models. While efforts have been made by some authors to use an adjustable VTEC scale factor (Montenbruck and Gill 2002; Hwang and Born 2005; Kim and Kim 2018), this approach is restricted to Kalman-filter based real-time navigation systems and cannot be used for the computation of pseudorange-based instantaneous position fixes. The same restriction applies for the use of an ionospheric-free code-carrier combination (Yunck 1993; Hwang and Born 2005; Montenbruck and Ramos-Bosch 2008; Bock et al. 2009) that can offer an almost complete compensation of ionospheric path delays in single-frequency navigation, but requires estimation of the unknown carrier phase ambiguities for each tracked satellite as part of the orbit determination process.

As an alternative to two-dimensional VTEC models, three-dimensional models of electron density lend themselves as an alternative for space users. By integrating the time- and location-dependent electron density along the ray path, the STEC can be determined for arbitrary user locations and viewing directions with no restrictions to the altitude of the receiver and the receiver-to-GNSS satellite geometry. Among the present and emerging GNSSs, Galileo is the first and only system that has adopted such a model for ionospheric correction in single-frequency positioning.

The NeQuick-G model (EC 2016) provides a three-dimensional description of electron density as a function of time, longitude, latitude and height as well as small set of ionospheric correction parameters that are continuously updated by the ground segment and transmitted to the Galileo users as part of the navigation message. Routine transmission of NeQuick-G ionosphere parameters started in April 2013 after launch of the first four in-orbit validation (IOV) satellites (Prieto-Cerdeira et al. 2014). The NeQuick-G model is targeted to reduce the residual ionospheric slant TEC error to less than 30% of the total STEC, or at least 20 TEC units (TECU), with a  $1\sigma$  (68%) probability over all observations (Prieto-Cerdeira et al. 2010; EC 2016). Tests ranging from the 2014 solar maximum to near minimum conditions (Orus Perez et al. 2018) have shown that the NeQuick-G model can in fact achieve the desired 70% correction capability in more than 80% of all cases and enables a 10–20% reduction of positioning errors compared to the Klobuchar model of GPS (Orus Perez 2017).

Based on the encouraging performance for terrestrial users and the three-dimensional nature of the NeQuick-G model, the present study assesses the STEC correction capability and positioning performance for spaceborne users based on comparison with measurements from a representative LEO satellite mission. Following this introduction, the basic concepts and properties of NeQuick-G are presented, and specific aspects of its application in low earth orbit are discussed. Thereafter, a summary of data and auxiliary products used in this study is provided. The actual data analysis and associated results are presented in the subsequent sections. These provide an evaluation of the STEC modeling performance of NeQuick-G in low earth orbit and the single-frequency positioning performance when using the full NeQuick-G STEC model. Finally, ionospheric mapping functions for spaceborne users are discussed and the positioning performance for a simplified slant TEC model is assessed, which uses the NeQuick-G VTEC along with a thick-layer mapping function.

## NeQuick-G model description and LEO application

NeQuick denotes a group of semiempirical, three-dimensional models for “quick” ionospheric electron density and total electron content (TEC) computation, which were developed by the Institute of Meteorology and Geophysics of the University of Graz and the Abdus Salam International Centre for Theoretical Physics, Trieste (Hochegger et al. 2000; Radicella and Leitinger 2001). Next to the original NeQuick-1 model, a refined NeQuick-2 version (Nava et al. 2008) and the Galileo-specific NeQuick-G (EC 2016) have

been released, which differ among others, in certain aspects of the top and bottomside density profile.

The vertical electron density distribution within the NeQuick models is generally described through a set of semi-Epstein layers (Rawer 1982), which are matched to the peak points of the  $E$ ,  $F_1$ , and  $F_2$  layers of the ionosphere. Each of the layers is described by its peak density and associated height as well as bottom and topside thickness parameters. Within the NeQuick models, these values are related to various ionosonde parameters, such as the critical frequency  $f_0F_2$  and the transfer parameter  $M3000(F_2)$ . Global maps of median values for these parameters were determined by the International Telecommunications Union (ITU) and its predecessor, the Comité Consultatif International des Radiocommunications (CCIR), based on actual measurements and represented in the form of a spherical harmonics approximation (Jones and Gallet 1962). These monthly ITU/CCIR maps serve as basis for describing seasonal, time-of-day, and geographic variations of the electron density in the NeQuick models.

Slant total electron content (STEC) in NeQuick is obtained by numerical integration of the electron density along the line of sight between the GNSS satellite and receiver. This requires computation and evaluation of the height-dependent electron density profiles above numerous foot points of the signal path and results in a computational effort that notably exceeds that of alternative two-dimensional ionosphere models (Klobuchar 1987, Hoque 2019). On the other hand, the three-dimensional nature of NeQuick imposes no height limitation and extends the range of application from the near-earth environment to spaceborne users.

Within NeQuick-1 and NeQuick-2, the dependence on solar activity is described through the  $F_{10.7}$  solar radio flux at 10.7 cm wavelength (in  $10^{-22} \text{ W m}^{-2} \text{ Hz}^{-1}$ ) or, equivalently,  $R_{12}$ , the average sun spot number. In NeQuick-G, this parameter is substituted by the effective ionization level

$$Az = a_{i0} + a_{i1}\mu + a_{i2}\mu^2 \quad (1)$$

where  $a_{i0}$ ,  $a_{i1}$ , and  $a_{i2}$  denote the ionospheric coefficients, which are broadcast as part of the navigation message (EU 2016). They are routinely determined within the Galileo ground segment by fitting the NeQuick-G model to STEC observations from a global ground station network. The modified dip latitude  $\mu$  in the above equation depends on the receiver's location. It is related to the geographic latitude  $\varphi$  and the magnetic inclination  $I$  through the defining relation

$$\tan(\mu) = \frac{I}{\sqrt{\cos(\varphi)}} \quad (2)$$

The magnetic inclination or dip is the angle of the geomagnetic field relative to the horizontal plane at the receiver position and is obtained in NeQuick-G from a suitable

magnetic field model using interpolation of tabulated values for a global grid of longitude/latitude points. By adjusting three independent parameters ( $a_{i0}$ ,  $a_{i1}$ ,  $a_{i2}$ ) to the ionospheric observations, the Galileo NeQuick model achieves a better global representation of the total electron content than would be possible with just a single  $Az$  value for all locations.

The comprehensive NeQuick-G algorithm description is provided in EC (2016) for users of the broadcast ionosphere parameters. A C++ software implementation of the model was developed by the present authors based on this specification and validated against the test cases given therein. For full consistency with the reference solutions, the Kronrod method from Annex F of EC (2016) was used for numerical integration of the electron density rather than the Gauss integration proposed in Sect. 2 of the same document. For completeness, we note that a reference software implementation of NeQuick-G is made available by the European Space Agency to registered and approved users as part of the European space software repository (<https://essr.esa.int/project/nequickg-galileo-ionospheric-correction-model>).

Other than NeQuick-1 and NeQuick-2, which directly use the solar flux or sun spot number as a proxy of the solar activity and associated level of ionization, the site-dependent effective ionization level  $Az$  must be evaluated when using the Galileo version of the NeQuick model.  $Az$  is not updated with the dip latitude along the line-of sight but fixed to the value of  $\mu$  at the receiver location. When applying NeQuick-G for space users, the conceptual problem of how to find the proper effective ionization level at altitudes well above the surface of the earth arises. Within NeQuick-G, the geographic variation of  $Az$  is described by (1), and the ionospheric coefficients ( $a_{i0}$ ,  $a_{i1}$ ,  $a_{i2}$ ) are designed to provide the best overall match of observed and modeled STEC values for users on or near the surface of the earth. In the absence of practical recommendations in the NeQuick-G specification (EC 2016), two different approaches can be imagined for LEO receivers:

- (a) The modified dip latitude for use in (1) is evaluated based on the geographic coordinates of the point at which the ray path from the GNSS satellite through the spaceborne receiver intersects the surface of the earth or comes closest to it.
- (b) The modified dip latitude  $\mu$  is evaluated based on the instantaneous geographic longitude and latitude of the spaceborne receiver.

The first option is based on the consideration that the resulting  $Az$  provides the best prediction of the entire ground-to-GNSS slant TEC value and the assumption that the same would hold for the fractional STEC between the LEO receiver and the GNSS satellite. The second option, in contrast, is conceptually and computationally simpler, but

cannot be expected to provide optimal results. Practical tests conducted with both formulations show only minor overall differences in the correction performance for a spaceborne user and, surprisingly, indicate a slight benefit for the second option. In view of this finding and the overall simplicity, we, therefore, applied option (b) in all analyses presented below.

## Data Sets

The NeQuick-G performance analysis for spaceborne GNSS receivers is based on data from the Swarm-C satellite. Swarm is a small-satellite constellation devoted to studies of the earth's magnetic field and atmosphere (Friis-Christensen et al. 2008). The three satellites orbit the earth in polar orbits of  $87^\circ$  inclination with mean altitudes of 480 km (Swarm-A and Swarm-C) and 520 km (Swarm-B) near the start of the mission in early 2014. Since then, the altitude of the lower pair has decreased by roughly 10 km per year.

The present analysis covers both a year of high solar activity (2014) and a year of low solar activity (2017). In each of these years, one day per month, i.e., day of year DOY 10, 40, ..., 340, is processed to include orbits with different local time of ascending node (LTAN). As a result of the earth's motion around the sun and the inertial drift of the orbital node, the LTAN of Swarm-C changes by roughly  $40^\circ$  (or 2.7 h) per month and therefore completes a full 24 h in about 9 months (Sieg and Diekmann 2016). For LTAN values near 2 h and 14 h the orbit passes through the electron density maximum of the ionospheric bulge, while the orbit is mostly confined to regions of low electron density for LTAN  $\sim$  8 h and 20 h (Fig. 2). With respect to geomagnetic activity, most test days represent quiet conditions with planetary  $K_p$  indices of 3 or less. In 2014, peak values of  $K_p = 4$  were only reached on two days (DOY 40 and 340). In 2017, increased geomagnetic activity was likewise encountered on two out of 12 test days. Here,  $K_p$  attained maximum values of 5 (DOY 190) and 8 (DOY 250), respectively.

All Swarm satellites are equipped with dual-frequency GPS receivers that can track up to eight GPS satellites concurrently and support precise orbit determination (van den Ijssel et al. 2015) as well as other science goals. They also serve as a basis for the Level-2 total electron content (TEC) product (Kervalishvili 2017), which provides observed slant TEC (STEC) and vertical TEC (VTEC) for the three Swarm satellites. STEC is obtained from the L1-L2 difference of code-leveled carrier phase observations after compensation of differential code biases as described in Noja et al. (2013). Differential code biases (DCBs) of the GPS are compensated in the TEC product generation using published values from the International GNSS Service (IGS), while receiver DCBs are estimated as part of a STEC-to-VTEC mapping with the

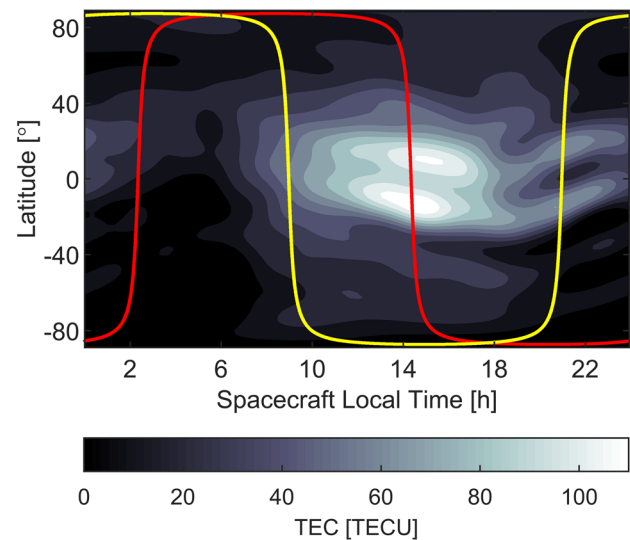


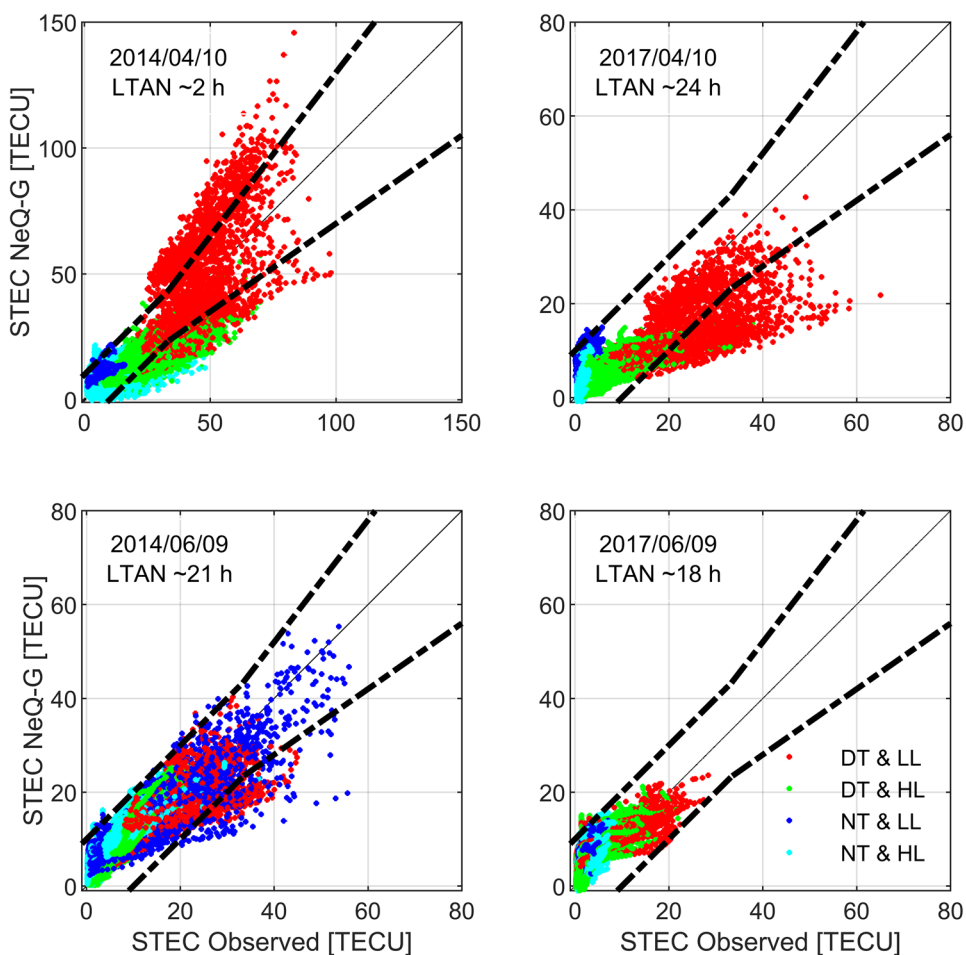
**Fig. 2** Ground track of Swarm-C on April 10, 2014 (red; LTAN  $\sim$  2 h) and June 9, 2014 (yellow; LTAN  $\sim$  21 h) as a function of spacecraft local time. For illustration, a map of terrestrial VTEC for 0 h UTC of April 10 is shown in the background based on data of the International GNSS Service

thick-layer mapping function of Foelsche and Kirchengast (2002).

Ionospheric correction parameters  $a_{i0}$ ,  $a_{i1}$ , and  $a_{i2}$ , for computing the effective ionization level  $A_z$  of the NeQuick-G model, are transmitted as part of the Galileo navigation message (EU 2016) and are generally included in the header of RINEX (Receiver INdependent EXchange format; IGS/RTCM 2019) navigation files collected by the IGS. Given the limited data coverage in early years of the IGS multi-GNSS network (Hoque et al. 2019), we made additional use of raw navigation data from the COoperative Network for GNSS Observations (CONGO, Montenbruck et al. 2011) to retrieve the respective parameters for the year 2014. It may be noted that ionospheric correction parameters may be updated more often than once per day in the Galileo navigation message, but only one randomly chosen set of daily values is typically made available in archived RINEX navigation data files. Accordingly, all tests reported in this work have been performed with just a single set per test day. No systematic quality assessment of sub-daily parameter sets has been done, but the impact of more frequent updates can be expected to be well within the overall uncertainty bounds of the NeQuick-G model and the scatter of ionospheric parameter estimates by the Galileo ground segment.

GPS measurements in the RINEX observation format are independently used within the present study to compute pseudorange-based single-point positioning (SPP) solutions of Swarm-C on the days of interest with different types of ionospheric corrections. Precise GPS orbit and clock solutions for this purpose are provided by the CODE Analysis

**Fig. 3** Comparison of modeled and observed/reference STEC values for GPS satellites tracked by the Swarm-C GPS receiver. Dashed lines mark a max (10 TECU, 0.3 STEC<sub>ref</sub>) error bound. Colors distinguish different regions in latitude and local time (DT: daytime 8–20 h, NT: nighttime, LL: low latitude (< 30°), HL: high latitude)



Center of the IGS (Dach et al. 2018). Group delay parameters for the signal-specific transformation of satellite clock offsets are taken from the IGS multi-GNSS DCB product of DLR (Montenbruck et al. 2014).

For comparison of the positioning performance with and without NeQuick-G corrections, pseudorange-based single-point positioning (SPP) solutions are compared against the precise science orbits (PSOs) of van den Ijssel et al. (2015). The PSOs are based on a reduced dynamic orbit determination using dual-frequency carrier phase observations and exhibit a representative 3D RMS accuracy of better than 5 cm, which is at least an order of magnitude better than that of the code-based single-point positioning solutions.

**Slant TEC**

The NeQuick-G model is expected to achieve a difference of less than 30% between observed and modeled slant TEC values or a maximum error of 20 TECU for small STEC for terrestrial users around the globe in at least 68% of all cases, when fed with the Galileo broadcast parameters

(Prieto-Cerdeira et al 2010; Orus Perez et al 2018). When evaluating the performance for spaceborne users, we likewise consider the same 30% relative error criterion but need to consider that STEC at the orbital altitude of the Swarm satellites is typically about one-half of the ground-based values. Therefore, we make use of a more stringent threshold of 10 TECU for the accepted absolute error at low STEC values.

Scatter plots of modeled vs. observed slant TEC values along the Swarm-C orbit for selected days in 2014 (high solar activity, left column) and 2017 (low solar activity, right column) are shown in Fig. 3. In accord with the coverage of the Swarm-C TEC product, all sample points are restricted to lines of sight above 20° elevation. Graphs in the top row represent cases in which the orbits pass through the ionospheric density maximum (Fig. 2). The lower row, in contrast, represents cases of high sun elevation above the orbital plane, where the Swarm-C satellite is mostly confined to regions of low electron density. Overall, the data points exhibit a balanced distribution around the symmetry line, even though systematic scaling errors in the NeQuick-G model can be recognized on individual days. These are most

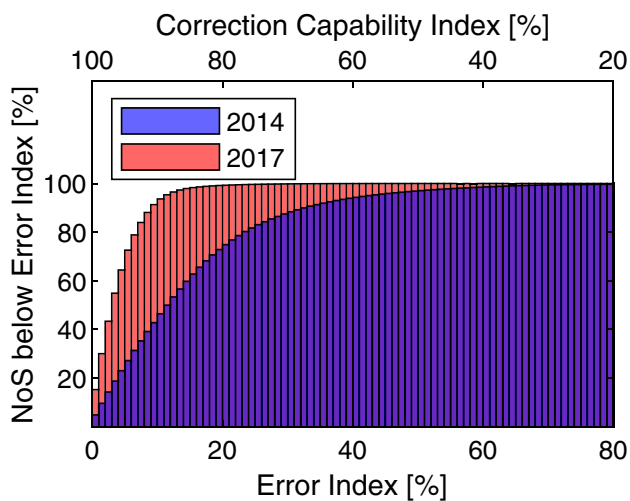


**Fig. 4** Cumulative distribution (number of samples, NoS) of NeQuick-G model errors along the Swarm-C orbit in 2014 and 2017

obvious in the year of low solar activity, where the model predictions appear to underestimate the actual STEC variation at daytime and low-latitude, i.e., in the vicinity of the ionospheric bulge. A degraded quality of NeQuick-G predictions at low-latitude regions, as compared to other regions, has earlier been noted in comparison of ground-based STEC observations as well as VTEC values from altimetry satellite missions (Hoque et al. 2019), which correlates with the present findings for a spaceborne GPS receiver.

Despite these obvious imperfections, most sample points fall within the corridor that marks a targeted error of less than 30% or 10 TECU.

To assess the NeQuick-G correction capability on a statistical basis, we follow the approach of Prieto-Cerdeira et al. (2014) and define the relative model error

$$\varepsilon = \text{RSS} \left( \frac{\text{STEC}_{\text{mod}} - \text{STEC}_{\text{ref}}}{\max(33\text{TECU}, \text{STEC}_{\text{ref}})} \right) \quad (3)$$

as the root sum square (RSS) of the relative error of the predicted STEC values over all samples. A dedicated 33 TECU limit is introduced to scale the relative error to 30% at 10 TECU model error for reference TECs below 10 TECU. The complementary value,  $1 - \varepsilon$ , describes the “correction capability”, i.e., the relative amount of ionospheric path delay that is removed when applying the NeQuick-G model.

The cumulative distribution of relative model errors obtained in this way is shown in Fig. 4 for the two years considered in the study. A relative error of less than 30%, or in other words, a 70% correction capability is achieved for 87% of all observations in a year of high (2014) solar activity and 98% in a year of low (2017) solar activity. This result is roughly comparable to the performance figures for

terrestrial users reported in Prieto-Cerdeira et al. (2010) and Orus Perez et al. (2018) and suggests that NeQuick-G can indeed be used to successfully correct ionospheric path delays in single-frequency GNSS positioning of orbiting platforms.

## Positioning performance

Using GPS observations and precise reference orbits of the Swarm-C satellite (van den Ijssel et al. 2015), we evaluate the accuracy of single-frequency SPP solutions with and without NeQuick-G corrections to assess the potential benefit of the model for LEO satellite navigation. For further reference, corresponding results are provided for SPP solutions using the ionosphere-free linear combination of L1 and L2 pseudoranges. To best reveal the impact of different ionospheric corrections on the positioning accuracy, precise GPS orbits and clock offset products are used in the computation of the SPP solutions instead of broadcast ephemerides. As such, all solutions are essentially free of signal-in-space range errors. These amount to roughly 0.5 m in the present GPS constellation and add to the user equipment errors such as receiver noise and multipath in an RSS sense (Montenbruck et al. 2018). All results are based on a  $10^\circ$  elevation mask, which is representative of actual space receiver configurations in missions with zenith pointing antennas and includes more low elevation observation than the STEC comparison presented in the previous section.

Throughout the Swarm mission, various configuration changes related to carrier phase smoothing, tracking loop bandwidths, and elevation mask have been applied to the GPS receivers (van den Ijssel et al. 2016), which impact the achievable SPP performance. Individual C/A-code and P(Y)-code pseudoranges of the Swarm GPS receiver exhibit an average noise level of about 15 cm in early 2014 but roughly 40 cm in 2017. A three times higher noise level of roughly 0.5 m and 1.2 m applies for the ionosphere-free combination of L1 and L2 pseudoranges in the respective years. At a representative position dilution of precision of 1.5 (2017) to 2.0 (2014), dual-frequency, single-point solutions of the Swarm satellites can thus attain a representative accuracy of 1.0–1.8 m when working with precise GPS ephemerides.

A timeline of single-frequency position errors for a 12 h sample data arc on April 10, 2014, is shown in Fig. 5. Without correction, RMS position errors of 6.3 m and peak errors of 28 m are obtained in an SPP solution based on L1 C/A-code pseudoranges. These errors reduce to 3.0 m and 11 m, respectively, when using the NeQuick-G model for the correction of ionospheric path delays. The model is particularly beneficial for the radial component, which is most sensitive to uncorrected path delays. As a rule of

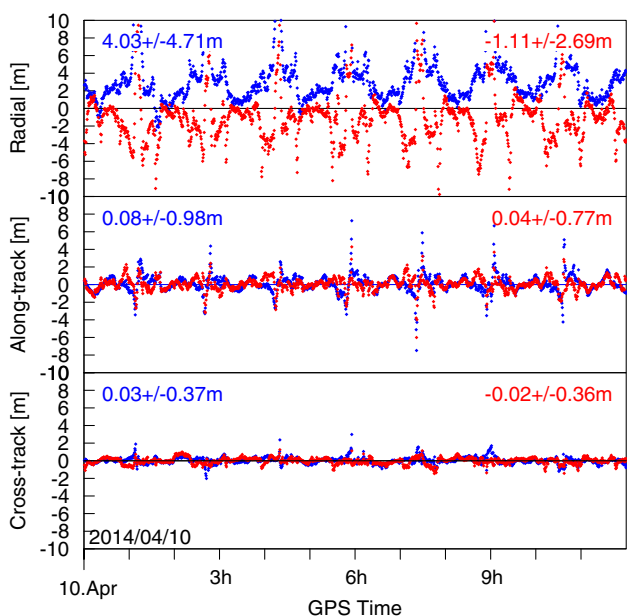


**Fig. 5** Swarm-C single-point positioning errors on April 10, 2014, using L1 C/A-code pseudoranges with (red) and without (blue) NeQuick-G correction of ionospheric path delays. Numbers in the upper left and right corners denote the corresponding mean ± 1σ errors

thumb, SPP solutions of orbiting receivers exhibit a mean radial bias of 5–7 times the uncompensated vertical delay for typical mask angles and elevation dependencies of the ionospheric delay (Garcia-Fernández and Montenbruck 2006). For the given test data set, a mean radial bias of +4 m can be observed, which changes to –1 m upon correction. Evidently, NeQuick-G overcompensates the actual path delays on average, but clearly removes the pronounced peak errors that arise once per revolution when the Swarm satellite passes the ionospheric density maximum.

In the case of an isotropic distribution of tracked satellites and a pure elevation dependence of the ionospheric path delays, the horizontal position is essentially unaffected by

ionospheric errors and the NeQuick-G correction has likewise little or no effect on the horizontal position accuracy. While a small ( about 20%) error reduction can still be recognized for the along-track component in the given test case, the error in the cross-track component is dominated by receiver noise and largely unaffected by ionospheric path delay errors.

A comparison of SPP errors for the selected test dates in 2014 and 2017 is provided in Fig. 6. The benefit of using NeQuick-G for correction of ionospheric delays in single-frequency positioning is most obvious in 2014, the year of high solar activity where the position errors can be reduced by a median value of 51%. In 2017, ionospheric path delays were notably smaller and the application of NeQuick results in a less pronounced, 17% median, reduction of the total positioning error. It is noteworthy, though, that the positioning errors of the NeQuick-G-corrected single-frequency solution turn out to be even slightly smaller in this year than those of the dual-frequency solution. The latter suffers from an increased noise level of the ionosphere-free combination, which slightly exceeds the contribution of NeQuick-G model errors during low solar activity.

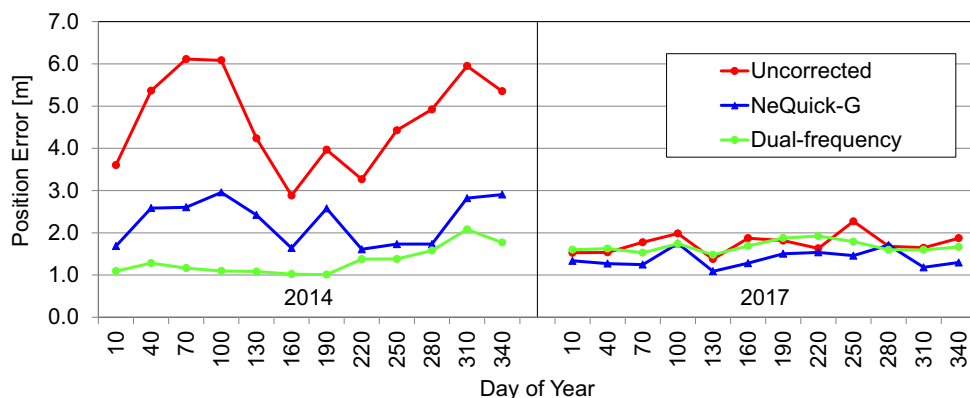
### Ionospheric mapping function for low earth orbits

For simplified modeling of ionospheric path delays, the slant total electron content (STEC) can be described by the product of the location-dependent vertical electron content (VTEC) and a mapping function  $m(E)$  that depends only on the elevation  $E$  of the line of sight from the receiver to the GNSS satellite:

$$STEC = m(E) \cdot VTEC \tag{4}$$

Assuming the idealized case of a spherically symmetric atmospheric shell of constant density and thickness  $h$  above a user at orbital radius  $r$ , the corresponding mapping function is given by

**Fig. 6** Accuracy of Swarm-C single-point positioning using L1 C/A-code pseudoranges with (blue) and without (red) NeQuick-G correction. For comparison, the green curve shows the accuracy of dual-frequency SPP solutions based on L1 C/A-code and L2 P(Y)-code observations



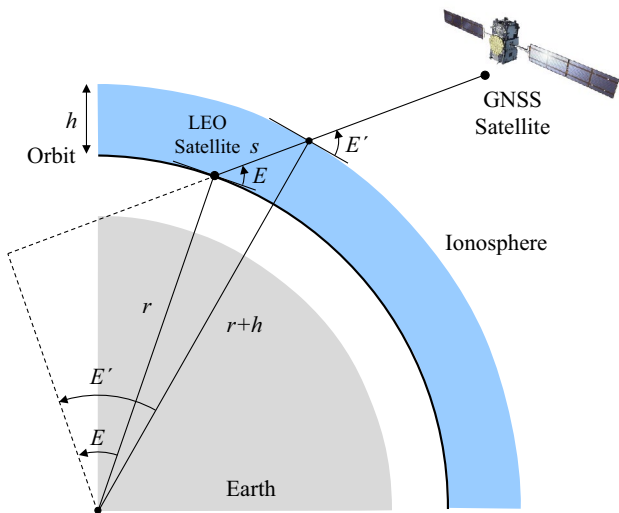


**Fig. 7** Derivation of the thick-shell ionospheric mapping function for LEO satellites

$$m(E) = \frac{s}{h} = \frac{1}{h} ((r + h)\sin E' - r \sin E) \tag{5}$$

(Fig. 7). Substituting the identity  $(r + h)\cos E' = r \cos E$ , the equivalent expressions

$$m(E) = \frac{2 + h/r}{\sqrt{\sin^2 E + \left(2 + \frac{h}{r}\right)\frac{h}{r}} + \sin E} \tag{6}$$

and

$$m(E) = \left(\frac{r}{h} + 1\right) \cos\left(\sin^{-1}\left(\frac{r}{r+h} \cos E\right)\right) - \frac{r}{h} \sin E \tag{7}$$

are obtained, which were independently suggested by Spilker (1996a,b) and Foelsche and Kirchengast (2002) for ionospheric and/or tropospheric path delay computation.

Following its early use within the COSMIC project (Syndergaard 2007; Yue et al. 2011), the F&K mapping function has been widely employed by the GPS radio occultation community for ionospheric TEC retrieval and differential code bias estimation in LEO missions (Noja et al. 2013; Wautelet et al. 2017; Watson et al. 2018; Li et al. 2019). Proposed values for the thickness  $h$  of the topside shell depend on the LEO satellite altitude and range from about 400–1000 km, and a thickness of twice the scale height is recommended in Foelsche and Kirchengast (2002). For the generation of the Swarm TEC product, the F&K mapping function is used with a thickness of  $h = 400\text{km}$  (Kervalishvili 2017).

For  $h/r = 0.037$ , which corresponds, for example, to a shell height of 250 km at an orbital altitude of 450 km

(Tancredi et al. 2011), the F&K mapping function attains the specific form

$$m(E) = \frac{2.037}{\sqrt{\sin^2 E + 0.076 + \sin E}} \tag{8}$$

which was first proposed by Lear (1989) for ionospheric correction of single-frequency GPS data of spaceborne receivers in the context of the US Space Station program. As described in Garcia-Fernández and Montenbruck (2006), the Lear mapping function closely matches the STEC/VTEC ratio at 450 km altitude for a Chapman density profile with 75 km scale height and peak electron density at 300 km altitude. Like the more generic F&K mapping function, the Lear mapping function has been widely employed for ionospheric correction of GPS observation from individual spacecraft as well as satellite formations (Garcia-Fernández and Montenbruck 2006; Tancredi et al. 2011).

A comparison of the Lear and F&K mapping functions, as well as thin-shell ionospheric mapping functions for LEO applications, is given in Zhong et al (2016). Overall the value of the mapping function at low elevation remains closer to one for increasing shell height and the dependence of the mapping function on the shell height is smaller for thick-shell models than for thin-shell models. To assess the overall realism of the slant TEC factorization in (4), the STEC/VTEC ratio as computed with the NeQuick-G model for Swarm-C is compared with the F&K mapping function in Fig. 8. Individual data points represent the STEC/VTEC ratio for the GNSS satellites observed by Swarm-C on the selected test days of 2014 and 2017 covering an elevation range of 20°–90°. The elevation-dependent median value of the distribution best matches the F&K thick-shell mapping function when assuming a thickness of about 900 km. For comparison, roughly 5% larger STEC/VTEC ratios are predicted by the F&K model for the 400 km shell height as adopted by Kervalishvili (2017). A notable scatter of the modeled STEC/VTEC ratios around the median value may be recognized from the 5th and 95th percentile lines in Fig. 8, which correspond to values of about 15–25% below and 30–50% above the median. The scatter largely reflects the fact that the actual slant TEC does not only depend on elevation but also varies with the azimuth angle of the line of sight. These variations can largely be attributed to horizontal gradients in the NeQuick-G electron density, which are not considered by the simplified STEC description of (4). On average over all data points, the NeQuick-G STEC/VTEC ratio shows a  $1\sigma$  scatter of about 25% with respect to the F&K mapping function. Accordingly use of a mapping function along with the local VTEC instead of the full, three-dimensional NeQuick-G model can be expected to result in a 25% degradation of the slant TEC modeling capability for spaceborne users.



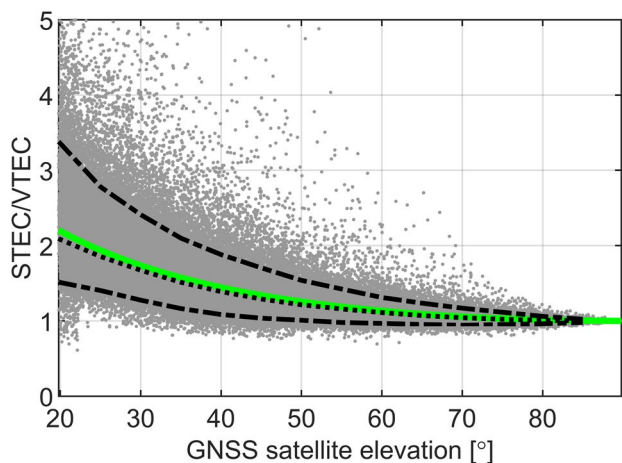


**Fig. 8** Comparison of STEC/VTEC values from the NeQuick-G model along the Swarm-C orbit in 2014 and 2017. Dashed black lines indicate the 5th and 95th percentile limits. The green line represents the F&K mapping function for a 900-km-thick shell above the Swarm orbit, which coincides with the elevation-dependent median of the STEC/VTEC ratio marked by a dotted line

### Positioning performance with simplified NeQuick-G

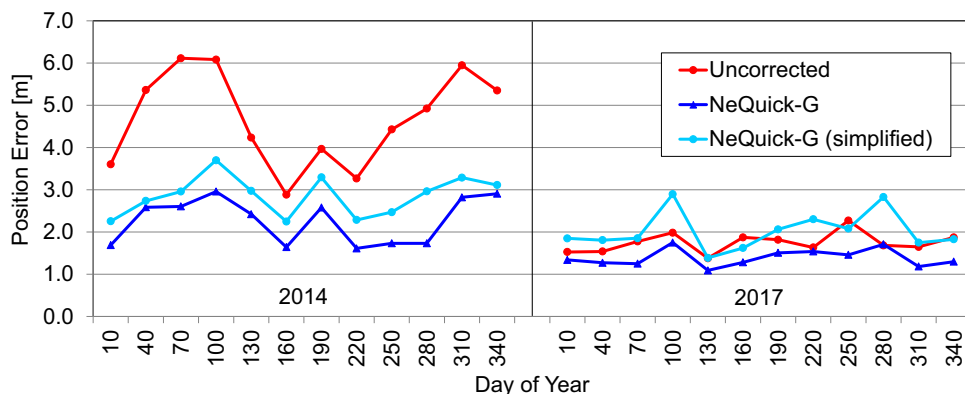
Even though a key benefit of NeQuick-G over other models lies in the fully three-dimensional description of the ionosphere, this advantage comes at the expense of a notably higher algorithmic complexity and computational load. Compared to ten equations that need to be evaluated for a single slant delay computation in the Klobuchar model of GPS (Klobuchar 1987, GPS Directorate 2019), the NeQuick-G specification comprises a total of 200 equations. Further more, these need to be evaluated independently for each grid point along the line of sight when integrating the slant TEC between the GNSS satellite and the receiver. Computation of a single NeQuick-G slant TEC value takes about 1 ms on a desktop computer, but ten, or even a hundred, times larger

values may apply for less-capable processors as used in representative space-hardened GNSS receivers. Compared to the evaluation of broadcast ephemerides and the computation of a least squares position solution without ionospheric correction, a more than 20-fold increase in computation time is observed with the present software implementation when incorporating the NeQuick-G model for slant delay computation. While receivers for terrestrial applications may evaluate the NeQuick-G model at a much lower update rate than the actual navigation solution to reduce the net computational load, the rapid motion of orbiting platforms mandates an update of the STEC values at each epoch.

With this background, simplified modeling using the slant TEC factorization into VTEC and mapping function as described in the previous section becomes of particular interest for the use of NeQuick-G in space applications. In the simplified formulation of (4), VTEC needs to be computed only once at the instantaneous user location and the evaluation of the mapping function (6) for each observed satellite represents a negligible effort. Accordingly, the computational load can be reduced by a factor equal to the number of satellites processed in the navigation solution. Obviously, this benefit comes at the expense of a degraded correction capability and reduced positioning accuracy.

A comparison of Swarm-C positioning accuracies obtained with the full and simplified formulation is provided in Fig. 9 for the selected test dates in 2014 and 2017. Evidently, the simplified model exhibits a reduced performance but still offers a 40% median correction in 2014 as may be expected from the quality of the mapping function discussed in the previous section. On the other hand, the use of the simplified NeQuick-G model during periods of low solar activity as in 2017 may even result in a degradation of the positioning accuracy compared to an uncorrected single-frequency solution.

**Fig. 9** Accuracy of Swarm-C single-point positioning using L1 C/A-code pseudoranges with full (dark blue) and simplified (light blue) NeQuick-G correction. For comparison, the red curve shows the single-frequency positioning accuracy without ionospheric correction



## Summary and conclusions

The fully three-dimensional nature of the NeQuick-G electron density model enables ionospheric correction of single-frequency GNSS observations at altitudes well above the surface of the earth. Using observed slant TEC values of the Swarm-C spacecraft, we have assessed the correction capability of the model for a low earth orbit satellite at an altitude of about 450 km. A better than 70% or, at least, 10 TECU correction is achieved for 87% of all observations in a year of high (2014) solar activity and 98% in a year of low (2017) solar activity. Positioning errors in the respective periods are reduced by 51% and 17% compared to an uncorrected single-frequency solution. The results confirm that the effective ionization level  $A_z$  of Galileo provides a suitable measure of total electron content for spaceborne receivers even though the ionospheric coefficients in the Galileo navigation message are optimized for use in terrestrial applications.

In view of the high computational effort implied by the complexity of the NeQuick-G model, a simplified formulation is studied, which factorizes the slant TEC into the product of the local vertical TEC above the user satellite and an elevation-dependent mapping function. A thick layer mapping function is shown to provide a reasonable approximation of the average STEC/VTEC ratio in the full NeQuick-G model and is therefore adopted in the simplified formulation. Depending on the actual number of simultaneously tracked GNSS satellites, the simplified model can offer an order of magnitude reduction in processing time. At high solar activity, a 40% reduction of position errors can be achieved in single-frequency solutions for Swarm-C with the simplified NeQuick-G model, but a slight degradation compared to uncorrected observations is observed during the low solar activity period. Nevertheless, the simplified formulation represents an interesting alternative for use in space receivers with limited resources and can provide reasonable corrections of ionospheric errors when needed most, i.e., at high solar activity. A decision on the use of a full implementation of NeQuick-G, the use of the simplified model or the use of uncorrected single-frequency observations can be taken at the receiver design stage or in actual operations depending on hardware capabilities and expected TEC values encountered in a specific mission.

**Acknowledgements** The authors would like to thank the European Space Agency and the Swarm Science Team for granting access to Swarm data and products that formed the basis for the present study. A Fortran version of the NeQuick-2 model, which served as a starting point and reference for the NeQuick-G implementation, has been made available by Bruno Nava of the Abdus Salam International Centre for Theoretical Physics, Trieste. His support and early discussions are greatly appreciated.

**Open Access** This article is distributed under the terms of the Creative Commons Attribution 4.0 International License (<http://creativecommons.org/licenses/by/4.0/>), which permits unrestricted use, distribution, and reproduction in any medium, provided you give appropriate credit to the original author(s) and the source, provide a link to the Creative Commons license, and indicate if changes were made.

## References

- Bock H, Jäggi A, Dach R, Schaer S, Beutler G (2009) GPS single-frequency orbit determination for low Earth orbiting satellites. *Adv Space Res* 43(5):783–791. <https://doi.org/10.1016/j.asr.2008.12.003>
- Dach R, Schaer S, Arnold D, Prange L, Sidorov D, Stegler P, Villiger A, Jaeggi A (2018) CODE final product series for the IGS. Published by Astronomical Institute, University of Bern. <https://www.aiub.unibe.ch/download/CODE>. <https://doi.org/10.7892/boris.75876.2>
- EC (2016) European GNSS (Galileo) Open Service—Ionospheric correction algorithm for Galileo single frequency users, Issue 1.2, Sept. 2016, European Commission
- EU (2016) European GNSS (Galileo) Open Service Signal in Space Interface Control Document, OS SIS ICD, Iss. 1.3, Dec. 2016, European Union
- Foelsche U, Kirchengast G (2002) A simple “geometric” mapping function for the hydrostatic delay at radio frequencies and assessment of its performance. *Geophys Res Lett* 29(10):111–1–111–4. <https://doi.org/10.1029/2001GL013744>
- Friis-Christensen E, Lühr H, Knudsen D, Haagmans R (2008) Swarm—an Earth observation mission investigating geospace. *Adv Space Res* 41(1):210–216. <https://doi.org/10.1016/j.asr.2006.10.008>
- García-Fernández M, Montenbruck O (2006) Low Earth orbit satellite navigation errors and vertical total electron content in single-frequency GPS tracking. *Radio Sci* 41(5), RS5001. <https://doi.org/10.1029/2005RS003420>
- GPS Directorate (2019) Navstar GPS space segment/navigation user segment interfaces. Interface specification IS-GPS-200, revision K, 4 March 2019, Global Positioning Systems Directorate
- Hochegger G, Nava B, Radicella S, Leitinger R (2000) A family of ionospheric models for different uses. *Phys Chem Earth Part C* 25(4):307–310. [https://doi.org/10.1016/S1464-1917\(00\)00022-2](https://doi.org/10.1016/S1464-1917(00)00022-2)
- Hoque MM, Jakowski N, Orús-Pérez R (2019) Fast ionospheric correction using Galileo  $A_z$  coefficients and the NTCM model. *GPS Solut* 23(2):41. <https://doi.org/10.1007/s10291-019-0833-3>
- Hwang Y, Born GH (2005) Orbit determination strategy using single-frequency global-positioning-system data. *J Spacecr Rockets* 42(5):896–901. <https://doi.org/10.2514/1.9573>
- IGS (2019) RINEX—the receiver independent exchange format, v. 3.04, Update 1, 26 April 2019; IGS RINEX Working Group and RTCM-SC104
- Jakowski N, Hoque MM, Mayer C (2011) A new global TEC model for estimating transionospheric radio wave propagation errors. *J Geodesy* 85(12):965–974. <https://doi.org/10.1007/s00190-011-0455-1>
- Jones WB, Gallet RM (1962) Representation of diurnal and geographic variations of ionospheric data by numerical methods. *J Res Natl Bureau Stand* 66D(4):419–438
- Kervalishvili G (2017) Swarm L2 TEC Product Description, SW-TR-GFZ-GS-0007, rev. 4, 22 May 2017, Swarm Expert Support Laboratories (ESL)

- Kim J, Kim M (2018) Orbit determination of low-earth-orbiting satellites using space-based augmentation systems. *J Spacecr Rockets* 55(5):1300–1302. <https://doi.org/10.2514/1.A34061>
- Klobuchar JA (1987) Ionospheric time-delay algorithm for single frequency GPS users. *IEEE Trans Aerosp Electron Syst* 23(3):325–331. <https://doi.org/10.1109/TAES.1987.310829>
- Lear WM (1989) GPS navigation for low-Earth orbiting vehicles, NASA 87-FM-2, JSC-32031, rev. 1, Lyndon B. Johnson Space Center, Houston, TX
- Li X, Ma T, Xie W, Zhang K, Huang J, Ren X (2019) FY-3D and FY-3C onboard observations for differential code biases estimation. *GPS Solut* 23(2):57. <https://doi.org/10.1007/s10291-019-0850-2>
- Montenbruck O, Gill E (2002) Ionospheric correction for GPS tracking of LEO satellites. *J Navig* 55:293–304. <https://doi.org/10.1017/S0373463302001789>
- Montenbruck O (2017) Space applications. In: Teunissen P, Montenbruck O (eds) *Springer Handbook of global navigation satellite systems*, Chapter 3. Springer, Berlin, pp 933–964
- Montenbruck O, Ramos-Bosch P (2008) Precision real-time navigation of LEO satellites using global positioning system measurements. *GPS Solut* 12(3):187–198. <https://doi.org/10.1007/s10291-007-0080-x>
- Montenbruck O, Hauschild A, Hessels U (2011) Characterization of GPS/GIOVE sensor stations in the CONGO network. *GPS Solut* 15(3):193–205. <https://doi.org/10.1007/s10291-010-0182-8>
- Montenbruck O, Hauschild A, Steigenberger P (2014) Differential code bias estimation using multi-GNSS observations and global ionosphere maps. *Navigation* 61(3):191–201. <https://doi.org/10.1002/navi.64>
- Montenbruck O, Steigenberger P, Hauschild A (2018) Multi-GNSS signal-in-space range error assessment—methodology and results. *Adv Space Res* 61(12):3020–3038. <https://doi.org/10.1016/j.asr.2018.03.041>
- Nava B, Coisson P, Radicella SM (2008) A new version of the NeQuick ionosphere electron density model. *J Atmos Solar Terr Phys* 70(15):1856–1862. <https://doi.org/10.1016/j.jastp.2008.01.015>
- Noja M, Stolle C, Park J, Lühr H (2013) Long-term analysis of ionospheric polar patches based on CHAMP TEC data. *Radio Sci* 48:289–301. <https://doi.org/10.1002/rds.20033>
- Orus Perez R (2017) Ionospheric error contribution to GNSS single-frequency navigation at the 2014 solar maximum. *J Geodesy* 91(4):397–407. <https://doi.org/10.1007/s00190-016-0971-0>
- Orus Perez R, Parro-Jimenez JM, Prieto-Cerdeira R (2018) Status of NeQuick G after the solar maximum of cycle 24. *Radio Sci* 53:257–268. <https://doi.org/10.1002/2017RS006373>
- Prieto-Cerdeira R, Binda S, Crisci M, Hidalgo I, Rodriguez D, Borrel V, Giraud J (2010) Ionospheric propagation activities during GIOVE Mission experimentation. In: *Proceedings of 4th European conference on antennas and propagation*, April 12–16, Barcelona
- Prieto-Cerdeira R, Orús-Pérez R, Breeuwer E, Lucas-Rodríguez R, Falcone M (2014) The European way—performance of the Galileo single-frequency ionospheric correction during in-orbit validation. *GPS World* 25(6):53–58
- Radicella SM, Leitinger R (2001) The evolution of the DGR approach to model electron density profiles. *Adv Space Res* 27(1):35–40. [https://doi.org/10.1016/S0273-1177\(00\)00138-1](https://doi.org/10.1016/S0273-1177(00)00138-1)
- Rawer K (1982) Replacement of the present sub-peak plasma density profile by a unique expression. *Adv Space Res* 2(10):183–190. [https://doi.org/10.1016/0273-1177\(82\)90387-8](https://doi.org/10.1016/0273-1177(82)90387-8)
- Sieg D, Diekmann F (2016) Options for the further orbit evolution of the Swarm mission. In: *Proceedings of living planet symposium*, SP-740, p 278
- Spilker JJ (1996a) GPS navigation data. In: Parkinson BW, Spilker JJ (eds) *Global Positioning System: theory and applications*, Chap. 4, vol 1. AIAA, Washington, pp 121–175
- Spilker JJ (1996b) Tropospheric effects on GPS. In: Parkinson BW, Spilker JJ (eds) *Global Positioning System: theory and applications*, Chap. 13, vol 1. AIAA, Washington, pp 517–546
- Syndergaard S (2007) FORMOSAT-3/COSMIC ionospheric data processing and availability for data assimilation systems. Presentation at the IUGG XXIV General Assembly, Perugia, Italy
- Tancredi U, Renga A, Grassi M (2011) Ionospheric path delay models for spaceborne GPS receivers flying in formation with large baselines. *Adv Space Res* 48(3):507–520. <https://doi.org/10.1016/j.asr.2011.03.041>
- van den Ijssel J, Encarnação J, Doornbos E, Visser P (2015) Precise science orbits for the Swarm satellite constellation. *Adv Space Res* 56(6):1042–1055. <https://doi.org/10.1016/j.asr.2015.06.002>
- van den Ijssel J, Forte B, Montenbruck O (2016) Impact of swarm GPS receiver updates on POD performance. *Earth Planets Space* 68(1):85. <https://doi.org/10.1186/s40623-016-0459-4>
- Watson C, Langley RB, Themens DR, Yau AW, Howarth AD, Jayachandran PT (2018) Enhanced Polar Outflow Probe ionospheric radio occultation measurements at high latitudes: receiver bias estimation and comparison with ground-based observations. *Radio Sci* 53(2):166–182. <https://doi.org/10.1002/2017RS006453>
- Wautelet G, Loyer S, Mercier F, Perosanz F (2017) Computation of GPS P1–P2 differential code biases with Jason-2. *GPS Solut* 21(4):1619–1631. <https://doi.org/10.1007/s10291-017-0638-1>
- Yuan Y, Wang N, Li Z, Huo X (2019) The BeiDou global broadcast ionospheric delay correction model (BDGIM) and its preliminary performance evaluation results. *Navigation* 66(1):55–69. <https://doi.org/10.1002/navi.292>
- Yue X, Schreiner WS, Hunt DC, Rocken C, Kuo YH (2011) Quantitative evaluation of the low Earth orbit satellite based slant total electron content determination. *Space Weather* <https://doi.org/10.1029/2011SW000687>
- Yunck TP (1993) Coping with the atmosphere and ionosphere in precise satellite and ground positioning. In: Valance-Jones A (ed) *Environmental effects on spacecraft trajectories and positioning*; AGU Monograph Series vol 73, pp 1–16. <https://doi.org/10.1029/GM073p0001>
- Zhong J, Lei J, Dou X, Yue X (2016) Assessment of vertical TEC mapping functions for space-based GNSS observations. *GPS Solut* 20(3):353–362. <https://doi.org/10.1007/s10291-015-0444-6>

**Publisher's Note** Springer Nature remains neutral with regard to jurisdictional claims in published maps and institutional affiliations.



**Oliver Montenbruck** is head of the GNSS Technology and Navigation Group at DLR's German Space Operations Center (GSOC). His research activities comprise spaceborne GNSS receiver technology, autonomous navigation systems, spacecraft formation flying and precise orbit determination as well as new constellations and multi-GNSS processing. Dr. Montenbruck presently chairs the Multi-GNSS Working Group of the International GNSS Service and coordinates the performance of

the MGEX Multi-GNSS Experiment. He is a fellow of the Institute of Navigation (ION) and received the ION Johannes Kepler Award in 2018.



**Belén González Rodríguez** is presently a Young Graduate Trainee at the European Space Research and Technology Centre (ESTEC) of the European Space Agency (ESA) in Noordwijk. She holds a bachelor's degree in aerospace engineering and air navigation from Universidad Rey Juan Carlos, Madrid, as well as a master's in astronautics and space engineering from Cranfield University.